Differential Effects of Substrate on Type I and Type II PKA Holoenzyme Dissociation†

Dominico Vigil,‡ Donald K. Blumenthal,§ Simon Brown,‡ Susan S. Taylor,‡ and Jill Trewhella*,‖

Department of Chemistry and Biochemistry and Howard Hughes Medical Institute, University of California at San Diego, La Jolla, California 92037, Departments of Pharmacology and Toxicology and Biochemistry, University of Utah, Salt Lake City, Utah 84112, and Bioscience Division, Los Alamos National Laboratory, Los Alamos, New Mexico 87545

Received January 9, 2004; Revised Manuscript Received March 6, 2004

ABSTRACT: It has been widely accepted that cAMP activates the protein kinase A (PKA) holoenzyme by dissociating the regulatory and catalytic subunits, thus freeing the catalytic subunit to phosphorylate its targets. However, recent experiments suggest that cAMP does not fully dissociate the holoenzyme. Here, we investigate this mechanism further by using small-angle X-ray scattering to study, at physiological enzyme concentrations, the type Iα and type IIβ holoenzyme structures under equilibrium solution conditions without any labeling of the protein subunits. We observe that while the addition of a molar excess of cAMP to the type Iα PKA holoenzyme causes partial dissociation, it is only upon addition of a PKA peptide substrate together with cAMP that full dissociation occurs. Similarly, addition of excess cAMP to the type IIβ holoenzyme causes only a partial dissociation. However, while the addition of peptide substrate as well as excess cAMP causes somewhat more dissociation, a significant percentage of intact type IIβ holoenzyme remains. These results confirm that both the type Iα and the type IIβ holoenzymes are more stable in the presence of cAMP than previously thought. They also demonstrate that substrate plays a differential role in the activation of type I versus type II holoenzymes, which could explain some important functional differences between PKA isoforms. On the basis of these data and other recently published data, we propose a structural model of type I holoenzyme activation by cAMP.

Protein phosphorylation, the process by which a protein kinase catalyzes the transfer of the γ-phosphate of ATP to a Ser, Thr, or Tyr residue in a target protein, is the most widespread method of reversible protein modification in eukaryotic cells. The cAMP-dependent protein kinase, or protein kinase A (PKA),[1] is ubiquitous in mammalian cells and is the most well-characterized member of the serine/threonine protein kinase family. Phosphorylation of its targets is known to be critical for regulating a multitude of cellular processes including metabolism, gene transcription, ion flux, growth, and cell death (*1*). The catalytic (C) subunits are responsible for catalyzing the phosphotransfer reaction, while the regulatory (R) subunits serve both to confer cAMP dependence and to localize the holoenzyme to discrete subcellular locations via interactions with A-kinase anchoring proteins (AKAPs) (*2*). There are two major isoforms of PKA, type I and type II, that differ with respect to their R subunits (RI or RII). At low cAMP concentrations, PKA is maintained as an inactive tetrameric (R_2C_2) holoenzyme consisting of a homodimeric R_2 subunit and two C subunits. When intracellular concentrations of cAMP increase in response to specific cellular stimuli, two cAMP molecules bind to each R subunit. This binding event is associated with the release of R subunit inhibition of C, allowing the C subunits to phosphorylate target proteins (*3*).

There is no doubt that cAMP binding lowers the affinity between R and C subunits, but how this occurs and whether it is sufficient for dissociation under equilibrium conditions similar to those found in the cell is of considerable importance. An understanding of the general mechanism of cAMP activation of PKA has great ramifications in cell biology, especially now as the importance of the spatial and temporal aspects of signal transduction are becoming better appreciated. The question of whether the PKA holoenzyme is dissociated by cAMP binding alone is especially critical to understanding the role of localization of PKA signaling by AKAPs.

It was widely accepted that cAMP activates PKA by causing C to physically dissociate from R. This mechanism

† This work was performed in part under the auspices of the U.S. Department of Energy (Contract W-7405-ENG-36) and in support of the Office of Science/BER Oak Ridge Structural Molecular Biology Center. Support for this work comes from the University of California Directed Research and Development (UCDRD) CULAR Grant 10005. D.V. is supported by a National Science Foundation Graduate Research Fellowship. Use of the Advanced Photon Source at Argonne National Laboratory was supported by the U.S. Department of Energy, Basic Energy Sciences (Contract W-31-109-ENG-38). BioCAT is a National Institutes of Health-supported Research Center RR-008630. An NIH Grant GM19301 to S.S.T. was also contributed.

* Corresponding author. Phone: (505) 667-2690. Fax: (505) 667-2670. E-mail: jtrewhella@lanl.gov.

‡ University of California.

§ University of Utah.

‖ Los Alamos National Laboratory.

[1] Abbreviations: AKAP(s), A-kinase anchoring protein(s); C, catalytic subunit of PKA; c, protein concentration; cAMP, cyclic adenosine monophosphate; D_{max}, maximum linear dimension; *M*, molecular weight; PKA, protein kinase A; R, regulatory subunit of PKA; R_2, regulatory subunit homodimer of PKA, R_g, radius of gyration; FRET, fluorescence resonance energy transfer; FPLC, fast performance liquid chromatography; SAXS, small-angle X-ray scattering; 8-AEA cAMP, 8-(2-aminoethyl) aminoadenosine-3′,5′-cyclic monophosphate; NHS, *N*-hydroxysuccinimide; cGMP, cyclic guanosine monophosphate; MES, 2-morpholinoethanesulfonic acid; DTT, dithiothreitol; EDTA, ethylenediaminetetraacetic acid; EGTA, ethylene glycol bis(β-aminoethyl ether)-*N*,*N*,*N*′,*N*′-tetraacetic acid; skMLCK, skeletal muscle myosin light chain kinase.

10.1021/bi0499157 CCC: $27.50
Published on Web 04/22/2004

was supported by a number of early in vitro experiments, including ion-exchange chromatography (*4*, *5*), gel filtration (*6*), and ultracentrifugation (*7*, *8*), which show that at low cAMP concentrations PKA exists as a holoenzyme complex, but at high cAMP concentrations the enzyme subunits dissociate into an R homodimer (R_2) and two C subunits. However, each of these experimental methods uses nonequilibrium conditions for the measurements (i.e., each exerts an artificial force upon the molecules that is not present under equilibrium conditions as might be present in the cell).

Evidence challenging this previously accepted mechanism of PKA activation is emerging. Data based on fluorescence resonance energy transfer (FRET) and fluorescence anisotropy measurements performed under equilibrium conditions (*9*, *10*) show that high levels of cAMP are insufficient to dissociate the type II holoenzyme. In addition, Døskelund and colleagues (*11*) have published the results of in vivo experiments that suggest undissociated type I holoenzyme can be present at high cAMP concentrations and that the cAMP-saturated holoenzyme is catalytically inactive toward its substrates. They also performed in vitro experiments and calculated the dissociation constant, K_D, between R and C subunits in the presence of cAMP to be about 0.2 μM and showed that the substrate could further destabilize the complex. Again, however, each of these experiments involved either labeling of protein or nonequilibrium conditions.

We have used small-angle X-ray scattering (SAXS) to further investigate the PKA dissociation mechanism and the effects of isoform differences (RIα vs RIIβ). The great sensitivity of SAXS to detect changes in protein associations gives us a direct and powerful method for monitoring the degree of PKA dissociation into separate R_2 and C components under stoichiometric and excess concentrations of cAMP, with cAMP plus substrate, and with substrate alone. Our experiments were done at 1.5 μM holoenzyme concentrations, close to what is considered to be the physiological concentration in many tissues even though localized pools of PKA could have much higher concentrations. For instance, the average intracellular concentration of PKA is estimated to be 1.2 μM in brain tissue, assuming the protein distributes in 70% of the intracellular space (*12*). Our experiments were performed under equilibrium solution conditions with no labeling and are therefore an excellent means to address the question of PKA dissociation with minimal potential experimental artifacts.

MATERIALS AND METHODS

Sample Preparation. Recombinant bovine C subunit was expressed and purified as described previously (*13*). Full-length bovine RIα and RIIβ subunits were expressed in *Escherichia coli* 222 and affinity purified on cAMP−Sepharose resin in which 100 μmol of 8-AEA cAMP (Biolog) was covalently coupled to 25 mL of NHS-activated Sepharose Fast Flow (Amersham Biotech) using the protocol supplied by the vendor. Five mL of resin was used per 2 L of cell culture. Three batch elutions (7 mL each) were performed at room temperature for 30 min each with buffer containing 25, 35, and 40 mM cGMP (Sigma), 20 mM MES, 100 mM NaCl, 2 mM EDTA, 2 mM EGTA, and 5 mM DTT, pH 5.6. Eluted fractions were pooled and then further purified using gel filtration (Superdex 200) in a buffer containing 50 mM MES, 200 mM NaCl, 2 mM EDTA, 2 mM EGTA, and 5 mM DTT. Type Iα and IIβ holoenzymes were formed by mixing purified R subunit with a molar excess of purified C and dialyzing against a buffer containing 2 mM $MgCl_2$ and 0.2 mM ATP, pH 7.0. These conditions approximate physiological concentrations for Mg^{2+}/ATP for most tissues. Gel filtration was then used to separate holoenzymes and heterodimer from free C. Holoenzyme and heterodimer activation by cAMP was checked with a coupled kinase assay to confirm that C subunit was inhibited in a cAMP-dependent manner (*14*). The substrate peptide, Kemptide, has the sequence LRRASLG and was synthesized by the Microchemical Facility of the University of California, Berkeley. cAMP was obtained from Sigma (St. Louis, MO).

X-ray Scattering Measurements. X-ray scattering data for the experiments performed using the type Iα holoenzyme (9.0 and 35 μM) and the type IIβ holoenzyme were acquired at 12 °C using the X-ray instrument at Los Alamos National Laboratory (*15*). Data were collected, reduced to $I(Q)$ versus Q, and analyzed as described previously (*15*). $I(Q)$ is the scattered X-ray intensity per unit solid angle, and Q is the amplitude of the scattering vector and is given by $4\pi(\sin\theta)/\lambda$, where 2θ is the scattering angle and λ is the wavelength of scattered X-rays (1.54 Å for this instrument). X-ray scattering data for the 1.5 μM concentration of type Iα holoenzyme sample were collected at 12 °C using the much higher intensities available at the BioCAT facility at the Advanced Photon Source (APS) at Argonne National Laboratory. The scattering station at this facility uses a sample holder with a water-jacketed flow cell that continuously flows sample back and forth in the beam to reduce X-ray damage at the high intensities used. A 3 m camera with a 49 × 86 mm, high-sensitivity CCD detector was used to collect scattered intensities at a wavelength of $\lambda = 1.03$ Å over a Q-range of 0.01−0.17 Å^{-1}. Data were reduced using the Fit2D software (*16*). The net scattered X-ray intensity for the protein was determined by subtracting a normalized buffer blank from each protein data set.

Calculation of Structural Parameters and Percent Dissociation. Structural information was derived from the scattering data by calculating the inverse Fourier transform of $I(Q)$, which yields $P(r)$, the probable frequency distribution of vector lengths, r, between scattering centers (atoms) within the scattering molecules (calculated using the program GNOM (*17*)). $P(r)$ provides insights into the overall shape of the scattering molecule with respect to its degree of symmetry or asymmetry and domain structure. $P(r)$ goes to zero at the maximum linear dimension, D_{max}, of the scattering particle, and its zeroth and second moments give the forward scattering, $I(0)$ and radius of gyration, R_g, respectively. The R_g value can also be estimated using a Guinier analysis (as described in ref *15*) in which the log of $I(Q)$ is plotted against Q^2 to yield a straight line whose slope is proportional to R_g. A nonlinear Guinier region is an indicator of nonspecific aggregation in the sample that would invalidate the analyses. The forward scattering, $I(0)$, is directly proportional to the product of the molar protein concentration and the average molecular weight squared of the scattering molecules. Forward scattering is therefore the strongest indicator of nonspecific aggregation. By comparing the forward scattering intensity extrapolated to zero protein concentration to that

of a known protein standard, one can determine to high precision whether there is any nonspecific aggregation present. Lysozyme standards were measured and compared to the forward scattering for PKA samples for all experiments performed at Los Alamos to determine the structural parameters under conditions for which we could demonstrate the holoenzymes were monodisperse.

For a two-component system, $I(0)$ is directly proportional to $c_1M_1^2 + c_2M_2^2$, where c_i and M_i are the molar concentration and molecular weight of component i. In the case of the type I PKA, the individual C subunits and the RIα homodimer have molecular weights of 40 490 and 85 500, respectively, and that of the holoenzyme is 166 500. Hence, the ratio of the observed $I(0)$ for a mixture of intact and partially dissociated holoenzyme ($I(0)_M$) to that expected if the holoenzyme were fully intact ($I(0)_U$) will be:

$$I(0)_M/I(0)_U = (c_1(85.5)^2 + 2c_1(40.49)^2)/c_2(166.5)^2 \quad (1)$$

The values of c_1 and c_2 are the molar concentrations of free RIα homodimer (R_2) and intact holoenzyme (R_2C_2), respectively. Note that there are two C subunits for each RIα homodimer; hence, the molar concentration of C is twice that of R_2 ($2c_1$). Percent dissociation, D, for the type Iα holoenzyme can be calculated from $I(0)_M$ and $I(0)_U$ by rearranging the previous equation

$$D = [c_1/c_2]\,100 = [1.62 - (1.62(I(0)_M))/I(0)_U]100 \quad (2)$$

Percent of intact holoenzyme is then simply $100 - D$. The possibility of a ternary complex (R_2C) is assumed to be insignificant to simplify the calculations. This assumption is justified in part by the known cooperativity between each R subunit in the activation process (*18*). Fully dissociated holoenzyme ($R_2 + 2C$) would give an $I(0)$ relative to intact holoenzyme of

$$(85.5^2 + 2(40.49)^2)/166.5^2 = 0.38$$

This relative $I(0)$ value is thus expected to be the lower limit for fully dissociated type Iα holoenzyme. The percent dissociation for the type IIβ holoenzyme is calculated in the identical way except using 92.4 kDa for the molecular weight of the R homodimer (R_2), yielding

$$D = [c_1/c_2]100 = [1.65 - (1.65(I(0)_M))/I(0)_U]100 \quad (3)$$

with fully dissociated holoenzyme giving an $I(0)$ relative to intact holoenzyme of

$$(92.4^2 + 2(40.49)^2)/173.4^2 = 0.39$$

RESULTS

Small-Angle Scattering Data and Structural Parameters for the Type Iα Holoenzyme with and without cAMP and Substrate Peptide. Scattering data were collected at three holoenzyme concentrations ranging from 1.5 to 35 μM and at various concentrations of cAMP and Kemptide substrate (Figure 1 and Table 1). Kemptide (*19*) is derived from a physiological PKA substrate and is an excellent choice of substrate for these experiments because it has K_m and V_{max} values that are as good as most physiological substrates, and its small size means that is does not contribute significantly

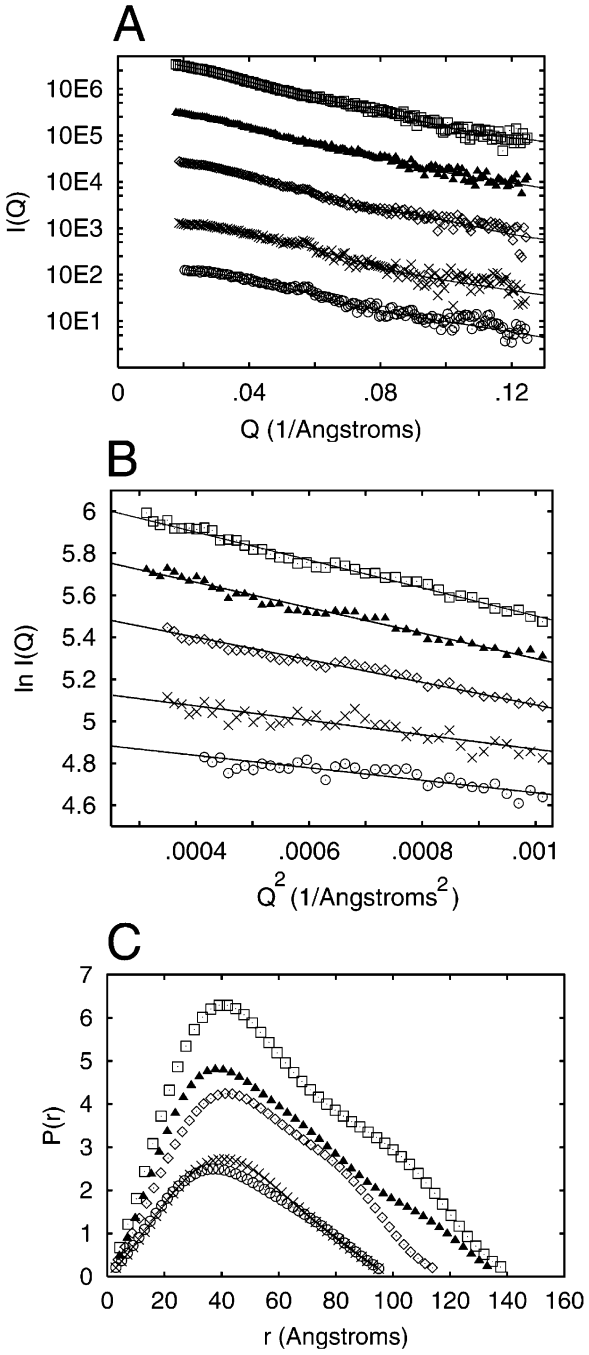

FIGURE 1: $I(Q)$ vs Q, Guinier, and $P(r)$ plots for cAMP/Kemptide titrations of the type Iα holoenzyme. (A) $I(Q)$ vs Q for 1.5 μM holoenyzme with no additions (open squares), with 6 μM cAMP (closed triangles), 1 mM cAMP (open diamonds), 6 μM cAMP + 1 mM Kemptide (crosses), and 1 mM cAMP + 1 mM Kemptide (open circles). Scattering profiles have been offset for comparison. Solid lines are the scattering profiles calculated using the program GNOM (*17*), from which the $P(r)$ functions in panel C and values in Table 1 are calculated. (B) Guinier plots of the cAMP/Kemptide titrations of the type Iα holoenzyme. Solid lines represent the best-fit lines through the Guinier region of the scattering profiles in panel A. Symbols are the same as those used in panel A. Guinier plots have been offset for ease of comparison. (C) Pair−distance distribution functions ($P(r)$ functions) for cAMP/Kemptide titrations of holoenzyme. Symbols are the same as used in panels A and B. Areas under the $P(r)$ curves reflect the square of the average molecular weight for the scattering particle and hence decrease as the holoenzyme dissociates. Note that cAMP addition to the holoenzyme causes a decrease in the average particle size, while cAMP and Kemptide together cause the average particle size to decrease even more. Estimated errors are smaller than the symbols.

Table 1: Structural Parameters for cAMP/Kemptide Titrations[a]

[holoenzyme]	[cAMP]	[Kemptide]	R_g (Å)	D_{max} (Å)	$I(0)$
Full-Length Type Iα Holoenzyme					
1.5	0	0	47.1 ± 0.5	140	100 ± 2
1.5	6	0	45.4 ± 0.5	140	74 ± 2
1.5	1000	0	41.6 ± 0.6	125	60 ± 2
1.5	6	20	36.7 ± 0.5	120	44 ± 2
1.5	6	1000	35.4 ± 0.7	100	33 ± 2
1.5	1000	1000	34.0 ± 1.0	100	29 ± 3
1.5	0	1000	48.3 ± 0.5	145	97 ± 2
9.0	0	0	52.9 ± 3.0	150	100 ± 4
9.0	2000	0	40.5 ± 2.0	120	59 ± 3
9.0	2000	2000	31.0 ± 2.0	100	36 ± 3
35.0	0	0	51.9 ± 1.5	143	100 ± 3
35.0	2000	0	43.7 ± 1.8	117	61 ± 2
35.0	2000	2000	35.3 ± 1.5	105	31 ± 2
Full-Length Type IIβ Holoenzyme					
10.0	0	0	46.2 ± 0.5	150	100 ± 2
10.0	1000	0	45.9 ± 1.0	135	59 ± 2
10.0	1000	1000	44.1 ± 0.7	135	52 ± 2

[a] Parameters are calculated as described in Materials and Methods. $I(0)$ values are normalized such that 100 is the $I(0)$ of the nondissociated holoenzyme for each holoenzyme concentration. [holoenzyme], [cAMP], and [Kemptide] are the concentrations of each of the indicated components in μM.

to the overall scattering intensity. In addition, its interactions with PKA are limited to the active site, which also simplifies mechanistic interpretation of the results. The scattering curves, Guinier plots, and $P(r)$ functions for the 1.5 μM holoenzyme and cAMP/Kemptide additions are shown in Figure 1A−C. The Guinier plots are all linear, consistent with the samples being free of nonspecific aggregation. The data from the lowest concentration samples collected at the higher intensity APS source yield slightly smaller R_g values and similar D_{max} values to those collected at higher protein concentrations at Los Alamos (Table 1) indicating that there is no significant radiation-induced aggregation in the APS data. The $P(r)$ function for the intact holoenzyme (Figure 1C) is asymmetric, with a peak around 40 Å, a shoulder around 100 Å, and a D_{max} of 140 Å suggestive of a bilobal, somewhat elongated structure similar to that observed previously for type IIα PKA (*20*), but with a more compact shape overall. The earlier IIα holoenzyme experiments used PKA reconstituted with a myristoylated C subunit, as compared to the nonmyristoylated recombinant C used in these experiments, and the consequent differences are discussed elsewhere (*21*).

The $P(r)$ functions in Figure 1C clearly show how the average particle size decreases with added cAMP and also that the maximal effect is observed only when both cAMP and Kemptide are present. The $I(0)$ measurements, together with the structural parameters R_g and D_{max} (Table 1), as well as the shape changes seen in the $P(r)$ functions, are consistent with the interpretation that only partial dissociation of the holoenzyme occurs at saturating cAMP concentrations, whereas full dissociation occurs with saturating cAMP levels plus peptide substrate. The R_g and D_{max} values become progressively smaller with added cAMP but then become even smaller with the addition of Kemptide substrate (Table 1). Importantly, at all three holoenzyme concentrations, the $I(0)$ value decreases with addition of cAMP but does not reach a minimum value until substrate peptide Kemptide is added as well. Because $I(0)$ would not change if the holoenzyme assumed a different conformation with no change in overall molecular weight, the large decreases in $I(0)$ seen with cAMP and Kemptide can only be explained by dissociation of the C subunits from the RIα homodimer. Addition of Kemptide alone did not significantly affect $I(0)$ or R_g, demonstrating that substrate is not sufficient to cause any dissociation of the holoenzyme.

On the basis of the known molecular weights of the holoenzyme and the individual subunits, one can estimate the percent holoenzyme dissociation using the observed $I(0)$ values and eq 2. These values are presented as a histogram in Figure 3A. Note that the $I(0)$ values actually level off when they are somewhat less than the theoretical lower limit (0.38 of the fully intact holoenzyme; see Materials and Methods), suggesting that dissociation may be accompanied by some loss of sample from the beam (e.g., through small amounts of precipitation).

Small-Angle Scattering Data and Structural Parameters for the Type IIβ Holoenzyme with and without cAMP and cAMP plus Kemptide. The scattering curves for the type IIβ holoenzyme with associated Guinier plots and $P(r)$ functions are shown in Figure 2A−C. The structural parameters derived from the scattering data are given in Table 1. The $P(r)$ function for the holoenzyme shows an overall globular shape, with a maximum of 50 Å and a D_{max} of 145 Å, similar to the type Iα holoenzyme in overall dimensions but without the pronounced shoulder at longer vector lengths. Upon addition of excess cAMP, the $P(r)$ becomes more asymmetric as its peak shifts to a smaller values of r (~30 Å) and D_{max} shrinks. The overall shape becomes indicative of a more extended rodlike structure. Addition of cAMP plus Kemptide shows some additional loss of intensity in the $P(r)$. There is little change in R_g accompanying these changes in $P(r)$ (Table 1 and Guinier plots). A recent small-angle scattering study of the isolated RIIβ homodimer shows it has a very extended, rodlike structure (*22*), consistent with the idea that the $P(r)$ function seen here is representative of a partially dissociated holoenzyme with free R_2 homodimer contributing to the observed average $P(r)$. The measured R_g value for the free C subunit ranges from 21 to 23 Å (*23*), while that for the free RIIβ homodimer is ~56 Å (*22*). Thus, upon dissociation, particles of both lower and higher R_g than the intact holoenzyme would be formed giving an average value, which appears coincidentally to be close to that of the holoenzyme. While R_g does not change, the normalized $I(0)$ after addition of excess cAMP drops to about 59% of its value as compared to the unliganded holoenzyme (Table 1 and Figure 3B). This result is consistent with a partial dissociation of the holoenzyme into free RIIβ homodimer and C subunits, with about 33% of the original holoenzyme remaining intact (Figure 3B and Materials and Methods). Upon addition of excess cAMP and Kemptide substrate, scattering parameters and the $P(r)$ function are very similar to what is seen when only cAMP is added. The normalized $I(0)$ is about 52% of what is seen in intact holoenzyme, signifying that about 21% of the holoenzyme remains intact (Table 1 and Figure 3B). Taken together, these results indicate that the type IIβ holoenzyme only partially dissociates upon cAMP binding, with somewhat more dissociation upon binding cAMP plus substrate, in contrast to the type Iα holoenzyme which fully dissociates upon binding cAMP plus substrate.

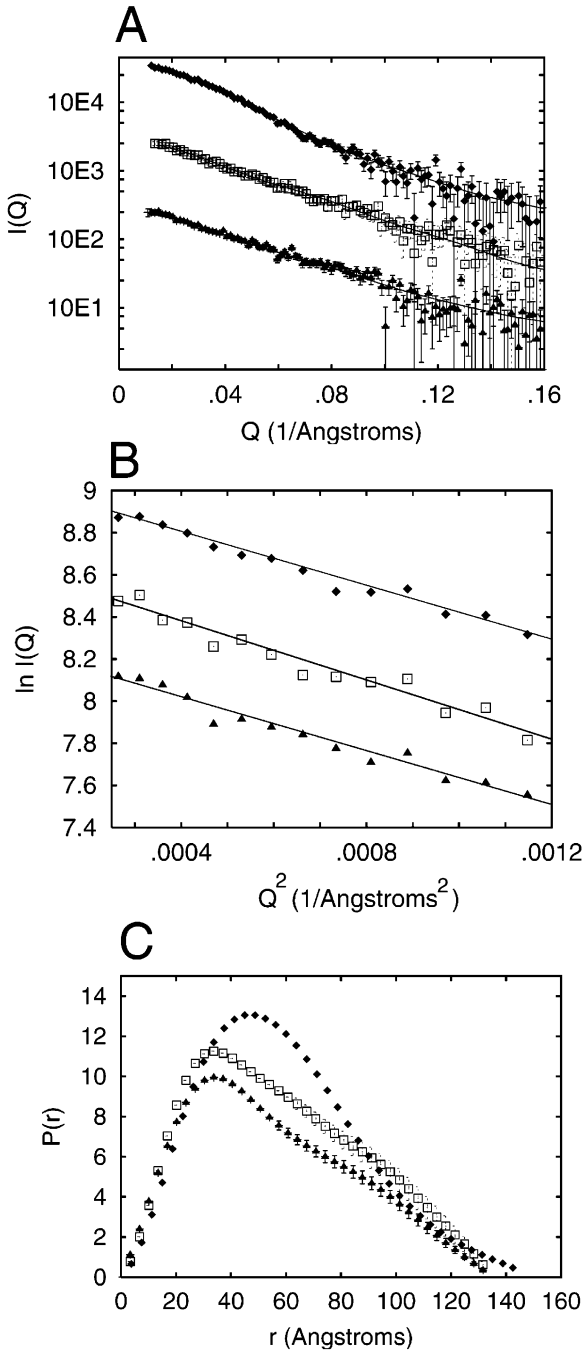

FIGURE 2: *I*(*Q*) vs *Q*, Guinier, and *P*(*r*) plots for cAMP/Kemptide titrations of the type IIβ holoenzyme. (A) *I*(*Q*) vs *Q* for the holoenzyme with no additions (closed diamonds), with 1000 μM cAMP (open squares), and with 1000 μM cAMP plus 1000 μM Kemptide (closed triangles). Solid lines are the scattering profiles calculated using the program GNOM (*17*), from which the *P*(*r*) functions in panel C and values in Table 1 are calculated. (B) Guinier plots of the cAMP/Kemptide titrations of the type IIβ holoenzyme. Solid lines represent the best-fit lines through the Guinier region of the scattering profiles in panel A. Symbols are the same as those used in panel A. (C) Pair−distance distribution functions (*P*(*r*) functions) for cAMP/Kemptide titrations of holoenzyme. Symbols are the same as used in panels A and B. Areas under the *P*(*r*) curves reflect the square of the average molecular weight of the scattering particles.

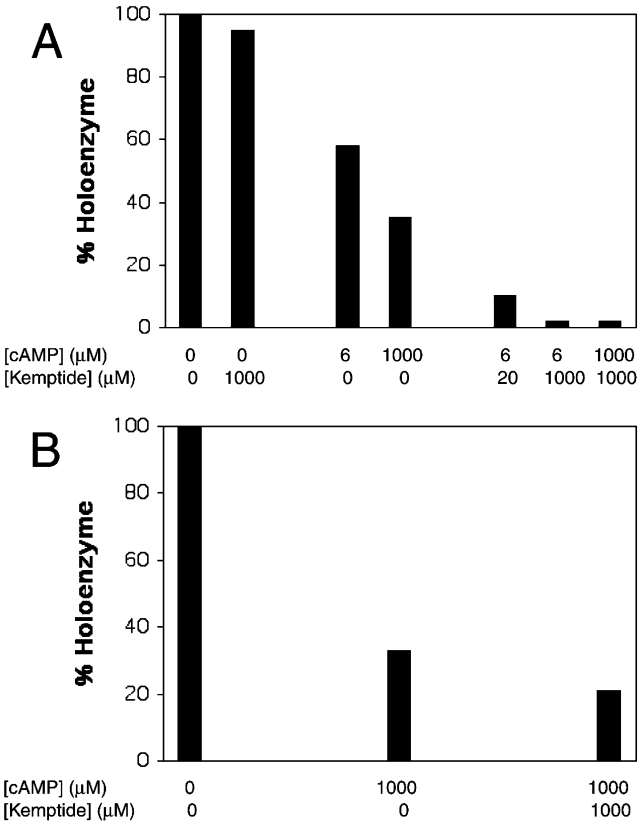

FIGURE 3: Histogram representation of the percent intact holoenzyme remaining after titration with cAMP/Kemptide. (A) Titrations of the type Iα holoenzyme. Values are calculated by equations given in Materials and Methods using the data obtained with 1.5 μM holoenzyme. It is clearly seen that cAMP alone causes partial dissociation, while cAMP and substrate cause full dissociation. Substrate alone has no measurable effect. (B) Titrations of the type IIβ holoenzyme. Note that a significant percentage of holoenzyme remains intact even after titration with excess cAMP and Kemptide.

DISCUSSION

Physiological Relevance of the Scattering Results. Whether or not PKA is activated by cAMP through a mechanism that involves dissociation of the R_2 and C subunits has wide-ranging physiological ramifications. Indeed, a dissociation mechanism seems at odds with recent reports indicating the important functional role of AKAPs in recruiting PKA to specific locations within the cell (*24*, *25*). A simple dissociation mechanism would lead to a delocalization of C subunit upon cAMP activation; thus, some of the benefit of PKA being localized to a subcellular site would be lost. On the other hand, it is known that increases in intracellular cAMP significantly increase concentrations of free C subunit in cells, especially in the nucleus (*26*), so some dissociation of holoenzyme by cAMP must occur. The recent studies by Døskelund and colleagues (*11*), as well as earlier fluorescence studies (*9*, *10*), suggest that the types I and II holoenzymes are much more stable in the presence of cAMP than previously thought. The results of the experiments presented herein confirm and extend this idea, using an equilibrium method that does not require any protein modifications. Although we are not able to calculate a dissociation constant from our data, our results indicate that at physiologically relevant concentrations of holoenzyme, in the absence of other associated proteins, there will be significant percentages of both intact holoenzyme and dissociated subunits when high concentrations of cAMP are present, in the case of both type I and type II isoforms. The significant fraction of C subunit that remains localized at high cAMP levels would allow prolonged spatial control of

PKA signaling, while also allowing some C subunit to diffuse to different subcellular compartments such as the nucleus.

Another interesting implication of these studies is that both the activation and the inactivation of PKA could occur much faster than in a simple dissociation mechanism. For the population of holoenzyme that does not dissociate when saturated with cAMP, activation would only involve an allosteric conformational change that is substrate dependent, not a cumbersome diffusion-limited dissociation step, thus allowing rapid activation by cAMP. The temporal effects on PKA inactivation would be expected to be even more significant. Inactivation of allosterically activated PKA would not require diffusion of C back to R_2. Moreover, cAMP dissociation from R_2 is much faster when C is bound to R_2 (*27*), allowing allosterically activated holoenzyme to be more rapidly deactivated and also facilitating rapid cAMP hydrolysis by proximal phosphodiesterases. It is interesting to note that phosphodiesterases have been identified in AKAP signaling complexes (*28*, *29*).

Døskelund et al. (*11*) reported that the cAMP-saturated type Iα holoenzyme complex was inactive toward substrate. However, we observed that addition of both cAMP and substrate to the type Iα holoenzyme causes full dissociation of R and C subunits, indicating that cAMP-saturated holoenzyme could be fully active toward substrate. It can be speculated that under the cellular conditions used in the previous study, other binding partners such as AKAPs influenced the activity of the holoenzyme. Because substrate induces delocalization of C from allosterically activated PKA, this might provide a plausible mechanism that limits hyperphosphorylation of substrates by PKA.

Perhaps the most interesting result in this study is that substrate does not play nearly as large a role in type IIβ holoenzyme dissociation as it does in type Iα. Types I and II R subunits share the same domain organization but differ in several biochemical properties. Importantly, it has been shown that Mg^{2+} and ATP regulate the stability of the type I but not the type II holoenzyme: two Mg^{2+} ions and high ATP concentrations are required for a tight type I holoenzyme complex (*30*). The differential effect of these cofactors on the stability of the holoenzyme could be directly related to the differential effect of substrate, but high-resolution structures of the R/C complexes will be necessary to test this idea. It has also been observed that in general, type II R subunits and holoenzymes are largely localized to specific subcellular locations, while localization of type I isoforms is more dynamic (*31*). In addition, the vast majority of known AKAPs bind type II but not type I R subunits (*32*). Our observation here that a significant population of type IIβ holoenzyme remains intact even after binding cAMP and substrate could be a result of the need for type II PKA to be more stably anchored. This also raises the possibility that a subset of type II PKA would remain localized even after activation and phosphorylation of targets such that multiple phosphorylation of different targets could be achieved in the same subcellular compartment. Type I PKA, on the other hand, would dissociate after the initial phosphorylation, preventing multiple phosphorylations of the same target or other substrates in the same subcellular compartment, leading to a fast and novel method for signal termination. Recently, a systems-level model of agonist-induced cardiac myocyte contraction was used to investigate the temporal role of PKA and other signaling components in this process (*33*). The experiments and hypotheses discussed previously, especially the differential kinetics of signal termination caused by dissociation of C from the holoenzyme between type I and type II, should be incorporated into such models, especially in the context of subcellular localization. Such an integration of structural biochemistry and systems-level analysis will likely provide biological insights into the design principles underlying signal transduction that would not be arrived at through the separate methods.

Structural Mechanism for Activation of Type I Holoenzyme. There are at least two major subsites of contact on RIα with the C subunit (*34*), one involving the RIα pseudosubstrate inhibitor region and a second involving the cAMP-binding domain A. Each site can bind individually to C with low affinity ($K_D = 1-10\ \mu M$), but both are necessary for high-affinity ($K_D = 0.2$ nM) binding to C. Two computational models of the R/C interaction have been developed using hybrid experimental data, and both predict a small peripheral R/C interface (<2000 Å) dominated by interactions with domain A of RIα (*35*, *36*). Recent molecular dynamics simulations (D. Vigil, unpublished experiments) and hydrogen/deuterium exchange experiments (*37*) also indicate that cAMP binding to RIα directly affects the conformation or accessibility of a specific helical region in cAMP-binding domain A. These observations, taken together with the present study, allow us to suggest a structural mechanism of activation that is illustrated in Figure 4. In this scheme, cAMP binding to RIα causes an allosteric conformational change in the R subunit subdomain of cAMP binding domain A that interacts with the C subunit such that the interactions are weakened. If a substrate is present, it competes with the pseudosubstrate inhibitor site and facilitates complete dissociation of the R−C complex. The demonstration that addition of substrate in the absence of cAMP to the holoenzyme does not cause dissociation or conformational changes suggests that the active site of C is completely blocked in the unactivated holoenzyme. However, cAMP binding to the holoenzyme causes a conformational change that allows substrate to compete with the pseudosubstrate inhibitor for the active site of C. The activation mechanism of type II holoenzyme appears to be somewhat more complicated since substrate is not as effective at competing with the pseudosubstrate region in this isoform.

Many protein kinases are regulated by protein/protein interactions involving both a pseudosubstrate inhibitor region and more distal regions (*38*). Our recent scattering studies of the calcium−calmodulin activation of skeletal muscle myosin light chain kinase (skMLCK) has revealed an interaction between that kinase and the N-terminal helix of calmodulin that is distinct from the autoinhibitory/pseudosubstrate interaction at the kinase active site but which is nevertheless required for activation. This distal interaction is implicated in enabling a translocation step that releases the autoinhibitory sequence (*39*). We have further shown that there is an additional conformational change in skMLCK and a reorientation of calmodulin with respect to the kinase catalytic domain upon substrate binding (*40*). The demonstration here that substrate plays a large role in the conformational changes associated with activation of the PKA holoenzyme suggests that substrates could play similar roles

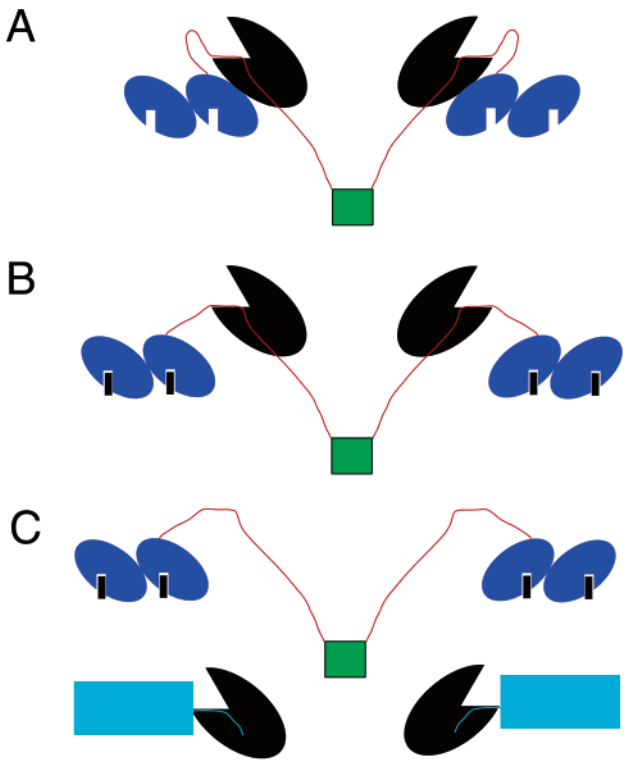

FIGURE 4: Cartoon representation of the proposed structural mechanism of cAMP activation of PKA. Catalytic subunits are represented as solid black "pac-man" shapes. For the R subunits, blue ellipses represent the A and B cAMP-binding subdomains, the green square represents the dimerization/docking domain, and the red line is the linker region that includes the pseudosubstrate inhibitor region. (A) Conformation of the holoenzyme at low cAMP concentrations. There are two sites of contact between R and C. One is the pseudosubstrate inhibitor region of R that binds to the active site cleft of C, and the other involves the cAMP-binding A of R and a distal region of the C subunit. (B) Conformation of the holoenzyme after cAMP binds (represented as small black rectangles). cAMP binding abolishes the peripheral contact site, but the pseudosubstrate inhibitor sequence remains bound to C. This lowers the affinity of R and C such that some C will dissociate but some will also remain bound to R. (C) When substrate (represented as the aqua object) comes into contact with the cAMP-activated holoenzyme, the substrate sequence competes with the pseudosubstrate inhibitor region of R for the C subunit, causing full dissociation of R and C subunits.

in the activation of many other protein kinases, whereby the full conformational change needed for kinase catalytic activation is achieved only when substrate competes with a pseudosubstrate inhibitor region or other associated proteins for the active site cleft.

ACKNOWLEDGMENT

We thank Brian Macdonald at Los Alamos National Laboratory and the staff at the Argonne National Laboratory BioCAT beamline for their expert technical assistance in collecting the scattering data. We thank Celina Juliano for purification of the C subunit.

REFERENCES

1. Walsh, D. A, Glass, D. B., and Mitchell, R. D. (1992) Substrate diversity of the cAMP-dependent protein kinase: regulation based on multiple binding interactions, *Curr. Opin. Cell Biol. 4*, 241−251.
2. Skälhegg, B. S., and Tasken, K. (2000) Specificity in the cAMP/PKA signaling pathway. Differential expression, regulation, and subcellular localization of subunits of PKA, *Front. Biosci. 5*, 678−693.
3. Johnson, D. A., Akamine, P., Radzio-Andzelm, E., Madhusudan, M., and Taylor, S. S. (2000) Dynamics of cAMP-depedent protein kinase, *Chem. Rev. 59*, 2243−2270.
4. Corbin, J. D., Brostrom, C. O., Alexander, R. L., and Krebs, E. G. (1972) Adenosine 3′,5′-monophosphate-dependent protein kinase from adipose tissue, *J. Biol. Chem. 247*, 3736−3743.
5. Rubin, C. S., Erlichman, J., and Rosen, O. M. (1972) Molecular forms and subunit composition of a cyclic adenosine 3′,5′-monophosphate-dependent protein kinase purified from bovine heart muscle, *J. Biol. Chem. 247*, 36−44.
6. Beavo, J. A., Bechtel, P. J., and Krebs, E. G. (1974) Preparation of homogeneous cyclic AMP-dependent protein kinase(s) and its subunits from rabbit skeletal muscle, *Methods Enzymol. 38*, 299−308.
7. Reimann, E. M., Walsh, D. A., and Krebs, E. G. (1971) Purification and properties of rabbit skeletal muscle adenosine 3′,5′-monophosphate-dependent protein kinase, *J. Biol. Chem. 246*, 1986−1995.
8. Tao, M., Salas, M. L., and Lipmann, F. (1970) Mechanism of activation by adenosine 3′,5′-cyclic monophosphate of a protein phosphokinase from rabbit reticulocytes, *Proc. Natl. Acad. Sci. 67*, 408−414.
9. Johnson, D. A., Leathers, V. L., Martinez, A. M., Walsh, D. A., and Fletcher, W. H. (1993) Fluorescence resonance energy transfer within a heterochromatic cAMP-dependent protein kinase holoenzyme under equilibrium conditions: new insights into the conformational changes that result in cAMP-dependent activation, *Biochemistry 32*, 6402−6410.
10. Yang, S., Fletcher, W. H., and Johnson, D. A. (1995) Regulation of cAMP-dependent protein kinase: enzyme activation without dissociation, *Biochemistry 34*, 6267−6271.
11. Kopperud, R., Christensen, A. E., Kjœrland, E., Viste, K., Kleivdal, H., and Døskeland, S. O. (2002) Formation of inactive cAMP-saturated holoenzyme of cAMP-dependent protein kinase under physiological conditions, *J. Biol. Chem. 277*, 13443−13448.
12. Hofmann, F., Bechtel, P. J., and Krebs, E. G. (1977) Concentrations of cyclic AMP-dependent protein kinase subunits in various tissues, *J. Biol. Chem. 252*, 1441−1447.
13. Slice, L. W., and Taylor, S. S. (1989) Expression of the catalytic subunit of cAMP-dependent protein kinase in *Escherichia coli*, *J. Biol. Chem. 264*, 20940−20946.
14. Cook, P. F., Neville, M. E., Jr., Vrana, K. E., Hartl, F. T., and Roskoski, R., Jr. (1982) Adenosine cyclic 3′,5′-monophosphate dependent protein kinase: kinetic mechanism for the bovine skeletal muscle catalytic subunit, *Biochemistry 21*, 5794−5799.
15. Heidorn, D. B., and Trewhella, J. (1988) Comparison of the crystal and solution structures of calmodulin and troponin C, *Biochemistry 27*, 909−915.
16. Hammersley, A. P., Svensson, S. O., Hanfland, M., Fitch, A. N., and Hausermann, D. (1996) Two-dimensional detector software: From real detector to idealized image or 2θ scan, *High-Pressure Res. 14*, 235−248.
17. Svergun, D. I., Semenyuk, A. V., and Feigin, L. A. (1988) Small-angle scattering data treatment by the regularization method, *Acta Crystallogr. A 44*, 244−250.
18. Herberg, F. W., Dostmann, W. R., Zorn, M., Davis, S. J., and Taylor, S. S. (1994) Crosstalk between domains in the regulatory subunit of cAMP-dependent protein kinase-influence of the amino-terminus on cAMP binding and holoenzyme formation, *Biochemistry 33*, 7485−7494.
19. Denis, C. L., Kemp, B. E., and Zoller, M. J. (1991) Substrate specificities for yeast and mammalian cAMP-dependent protein-kinases are similar but not identical, *J. Biol. Chem. 266*, 17932−17935.
20. Zhao, J., Hoye, E., Boylan, S., Walsh, D. A., and Trewhella, J. (1998) Quaternary structures of a catalytic subunit-regulatory subunit dimeric complex and the holoenzyme of the cAMP-dependent protein kinase by neutron contrast variation, *J. Biol. Chem. 273*, 30448−30459.
21. Heller, W. T., Vigil, D., Brown, S., Blumenthal, D. K., Taylor, S. S., and Trewhella, J. (2004) C subunits binding to the protein kinase A RIα dimer induce a large conformational change, *J. Biol. Chem*, in press.
22. Vigil, D., Blumenthal, D. K., Heller, W. T., Brown, S., Canaves, J. M., Taylor, S. S., and Trewhella, J. (2004) Conformational

differences among solution structures of the type Iα, IIα, and IIβ protein kinase A regulatory subunit homodimers: role of the linker regions, *J. Mol. Biol*. *337*, 1183−1194.
23. Olah, G. A., Mitchell, R. D., Sosnick, T. R., Walsh, D. A., and Trewhella, J. (1993) Solution structure of the cAMP-dependent protein kinase catalytic subunit and its contraction upon binding the protein kinase inhibitor peptide, *Biochemistry 32*, 11326−11334.
24. Rubin, C. S. (1994) A-kinase anchor proteins and the intracellular targeting of signals carried by cyclic-AMP, *Biochim. Biophys. Acta 1224*, 467−479.
25. DellAcqua, M. L., and Scott, J. D. (1997) Protein kinase A anchoring, *J. Biol. Chem. 272*, 12881−12884.
26. Adams, S. R., Harootunian, A. T., Buechler, Y. J., Taylor, S. S., and Tsien, R. Y. (1991) Fluorescence ratio imaging of cyclic-AMP in single cells, *Nature 349*, 694−697.
27. Houge, G., Steinberg, R. A., Ogreid, D., and Døskeland, S. O. (1990) The rate of recombination of the subunits (RI and C) of cAMP-dependent protein kinase depends on whether one of two cAMP molecules are bound per RI monomer, *J. Biol. Chem. 265*, 19507−19516.
28. Dodge, K. L., Khouangsathiene, S., Kapiloff, M. S., Mouton, R., Hill, E. V., Houslay, M. D., Langeberg, L. K., and Scott, J. D. (2001) mAKAP assembles a protein kinase A/PDE4 phosphodiesterase cAMP signaling module, *EMBO J. 20*, 1921−1930.
29. Tasken, K., Collas, P., Kemmner, W. A., Witczak, O., Conti, M., and Tasken, K. (2001) Phosphodiesterase 4D and protein kinase A type II constitute a signaling unit in the centrosomal area, *J. Biol. Chem. 276*, 21999−22002.
30. Herberg, F. W., and Taylor, S. S. (1993) Physiological inhibitors of the catalytic subunit of cAMP-dependent protein kinase-effect of MgATP on protein−protein interactions, *Biochemistry 32*, 14015−14022.
31. Scott, J. D. (1991) Cyclic nucleotide-dependent protein kinases, *Pharmacol. Ther. 50*, 123−145.
32. Michel, J. J. C., and Scott, J. D. (2002) AKAP mediated signal transduction, *Annu. Rev. Pharmacol. 42*, 235−257
33. Saucerman, J. J., Brunton, L. L., Michailova, A. P., and McCulloch, A. D. (2003) Modeling β-adrenergic control of cardiac myocyte contractility in silico, *J. Biol. Chem. 278*, 47997−48003.
34. Huang, L. J. S., and Taylor, S. S. (1998) Dissecting cAMP binding domain A in the RIα subunit of cAMP-dependent protein kinase-Distinct subsites for recognition of cAMP and the catalytic subunit, *J. Biol Chem. 273*, 26739−26746.
35. Tung, C.-S., Walsh, D. A., and Trewhella, J. (2002) A structural model of the catalytic subunit−regulatory subunit dimeric complex of the cAMP-dependent protein kinase, *J. Biol. Chem. 277*, 12423−12431.
36. Anand, G. S., Law, D., Mandell, J. G., Snead, A. N., Tsigelny, I., Taylor, S. S., Ten Eyck, L. F., and Komives, E. A. (2003) Identification of the protein kinase A regulatory RIα-catalytic subunit interface by amide H/H-2 exchange and protein docking, *Proc. Natl. Acad. Sci. U.S.A. 100*, 13264−13269.
37. Anand, G. S., Hughes, C. A., Jones, J. M., Taylor, S. S., and Komives, E. A. (2002) Amide H/H-2 exchange reveals communication between the cAMP and catalytic subunit binding sites in the RIα subunit of protein kinase A, *J. Mol. Biol. 323*, 377−386.
38. Huse, M., and Kuriyan, J. (2002) The conformational plasticity of protein kinases, *Cell 109*, 275−282.
39. Krueger, J. K., Gallagher, S. C., Zhi, G., Geguchadze, R., Persechini, A., Stull, J. T., and Trewhella, J. (2001) Activation of myosin light chain kinase requires translocation of bound calmodulin, *J. Biol. Chem. 276*, 4535−4538.
40. Krueger, J. K., Zhi, G., Stull, J. T., and Trewhella, J. (1998) Neutron scattering studies reveal further details of the Ca^{2+}/calmodulin-dependent activation mechanism of myosin light chain kinase, *Biochemistry 37*, 13997−14004.

BI0499157